

Hartree and Jastrow approximations for monolayer solids of Ne, D₂, H₂, ⁴He, and ³He

X. -Z. Ni and L. W. Bruch

Department of Physics, University of Wisconsin-Madison, Madison, Wisconsin 53706

(Received 4 November 1985)

Calculations are reported for monolayer solids of Ne, D₂, H₂, ⁴He, and ³He, with Hartree and Jastrow approximations for Lennard-Jones potential models in mathematical two dimensions. Estimates are made for the energies of solids at condensation, for enthalpies of the compressed solids, for the highest densities which can be reached for adsorption on the basal plane surface of graphite and on the (111) face of silver, and for energies of registry $\sqrt{3}$ lattices on graphite. Melting of the monolayer solids of helium is treated.

I. INTRODUCTION

There are several reasons for a renewed interest in the theory of monolayer solids with large quantum effects. Atom-surface scattering experiments¹⁻⁵ have improved the knowledge of the holding potential for light adsorbates such as helium and hydrogen. The large compressions of the monolayer solids of helium⁶ and of hydrogen⁷ on basal plane graphite which are achieved before further layer condensation make these systems significant for general discussions⁸ of the conditions which may lead to limited layer growth in physisorption. For helium adsorption with a weak holding potential, as on hydrogen films,⁹ there is a question whether the limiting state of the monolayer is a liquid or solid. In the physical adsorption of H₂ on a smooth surface such as the (111) face of silver,⁵ H₂/Ag(111), the system may be close to the regime where a quantum system at very low temperatures condenses as a liquid rather than as a solid. We report here the results of calculations using the Hartree and Jastrow variational approximations to the quantum mechanics of two-dimensional systems, with estimates of energies and lattice constants for several adsorbate/substrate combinations of recent experiments.

The most systematic theoretical study of the relative stability of solid, liquid, and gas phases at very low temperatures, for light atomic masses, has been the elaboration of the quantum-mechanical law of corresponding states by Nosanow and co-workers.^{10,11} They used the Jastrow variational theory and Lennard-Jones pair potentials for the interactions among the atoms. We extend their results by determining the critical de Boer parameter in two dimensions where the ground-state energy of the boson liquid becomes equal to that of the solid.

Nosanow and Shaw¹² developed the Hartree approximation for the three-dimensional inert gas solids. Novaco^{13,14} performed Hartree calculations for monolayer solids of helium, both for mathematical two dimensions and with allowance for vibrations perpendicular to the substrate for helium adsorbed on graphite. We report extensive calculations for the Hartree approximation to

Lennard-Jones systems in two dimensions. Novaco's work for He on graphite is updated by use of holding potential parameters derived from atomic scattering experiments¹ and there is an application³ to ⁴He/Ag. Calculations for the D₂ and H₂ parameters lead to estimates for the limit of monolayer compression in adsorption on graphite⁷ and on Ag(111),⁵ the first theoretical treatment of the limit for these systems. The energetic stability of the $\sqrt{3}R$ 30° lattices of D₂, H₂, ⁴He, and ³He on graphite is also treated, and there are estimates for an Einstein oscillator frequency of the $\sqrt{3}$ lattices of D₂ and H₂ on graphite.¹⁵

Liu *et al.*¹⁶ examined the melting transition of two-dimensional ⁴He using Jastrow variational calculations. We extend their work to other de Boer parameters, and find some changes in the ⁴He melting parameters. The Jastrow results are also used to calculate the zero-temperature equation of state of the compressed quantum monolayer solids.

Monolayer solids of neon have been treated^{17,18} with approximations which lead to 5% differences in the lateral ground-state energy. We use the Hartree and Jastrow approximations for a Lennard-Jones potential model and determine the ground-state energy to 1% for the given model, thus clarifying the relation among the various approximations for neon.

The organization of this paper is as follows. Section II A contains a summary of the interatomic potentials and adsorption and cohesive energies which are used in the calculations; Sec. II B contains a review of the approximation techniques for calculating the energy of a quantum monolayer. The applications are contained in Sec. III. An overview of the results is presented in Tables III and IV. Section IV contains some concluding remarks. There are two Appendices: Appendix A contains a summary of a variation-perturbation approximation to the Hartree theory which has good accuracy for neon and is a useful preliminary to detailed calculations for D₂; Appendix B contains a summary of lattice dynamical calculations on the bilayer condensation of D₂ on graphite and comments on a possible structural reorganization¹⁹ of the bilayer into an oblique unit cell.

II. COMPONENTS OF THE CALCULATIONS

A. Interaction models and cohesive energies

1. Adsorbate-adsorbate interactions

We take the adsorbate-adsorbate (inert gas atom-atom and molecule-molecule) interactions to be given by Lennard-Jones (12,6) pair potentials:

$$\begin{aligned}\phi(r) &= 4\epsilon[(\sigma/r)^{12} - (\sigma/r)^6] \\ &= \epsilon[(R_0/r)^{12} - 2(R_0/r)^6],\end{aligned}\quad (2.1)$$

with parameters given in Table I. Properties calculated with the de Boer–Michels²⁰ Lennard-Jones potential for helium are close to those for more complex multiparameter potential models.^{21–23} The Lennard-Jones potential model for the isotopic hydrogen series²⁴ omits anisotropic interaction terms and is a more primitive model,²⁵ but it leads to values²⁶ for the ground-state energy and lattice constant of the three-dimensional (3D) solids which are close to the experimental values.²⁵ The parameters for neon also reproduce properties of the 3D ground state rather well.^{27,28}

The adsorbed H₂ and D₂ are modeled here as spherically symmetric objects, although small departures from free 3D rotor states are observed⁵ for H₂/Ag(111) and D₂/Ag(111).

The de Boer parameter for atoms (molecules) of mass m interacting through the Lennard-Jones (12,6), LJ(12,6), potential is

$$\Lambda^* = h / (\sigma \sqrt{m\epsilon}), \quad (2.2)$$

where h is Planck's constant. A second form of this parameter used by Nosanow and co-workers¹⁰ is

$$\eta = [\Lambda^* / (2\pi)]^2. \quad (2.3)$$

Dimensionless energies, densities, spreading pressures, and enthalpies are constructed with the energy and length scales of the Lennard-Jones potential by

$$E^* = E/\epsilon, \quad \rho^* = \rho\sigma^2, \quad p^* = p\sigma^2/\epsilon, \quad (2.4)$$

$$h^* = E^* + (p^*/\rho^*).$$

There are several advantages for the computations arising

TABLE I. Lennard-Jones (12,6) potential parameters. ϵ (in K) and σ (in Å) of the LJ(12,6) potential function, Eq. (2.1); de Boer parameter Λ^* defined in Eq. (22).

System	ϵ (K)	σ (Å)	Λ^*
²⁰ Ne ^a	36.76	2.786	0.579 42
D ₂ ^b	36.7	2.958	1.216
H ₂ ^b	36.7	2.958	1.720
⁴ He ^c	10.22	2.556	2.67
³ He ^c	10.22	2.556	3.08

^aFrom Ref. 27.

^bFrom Ref. 24, neglecting the distinction between parameters for D₂ and H₂.

^cFrom Ref. 20.

from the simplicity of the Lennard-Jones form, Eq. (2.1). In the Hartree calculations, we perform two angular integrations analytically. In the Jastrow calculations, McMillan scaling²⁹ greatly reduces the number of Monte Carlo simulations required for the variational searches. Putting results for the two-parameter Lennard-Jones form into the format of the quantum-mechanical law of corresponding states¹⁰ provides a way to follow systematic trends of the quantum effects and to construct interpolations for other cases.

We do not explicitly include the several adsorption-induced modifications to adsorbate-adsorbate interactions which are known³⁰ to yield 10% to 20% adjustments in the lateral energies of inert gases on graphite and on Ag(111). Estimates of these effects may be obtained by fitting an LJ(12,6) potential to the net pair potential and then interpolating in our results.

The distinction²⁴ in the Lennard-Jones parameters for H₂ and D₂ is omitted. The Michels values for D₂ would lead to a de Boer parameter differing by 2% from the value in Table I; the effect of such adjustments can be estimated by interpolating in our results. Anisotropic components²⁵ of the molecule-molecule interaction are omitted although they are significant for the orientationally aligned phases of the 3D solids and of ortho-H₂ on graphite³¹ and may be significant for the structure of the compressed monolayer (see also Appendix B).

2. Adsorbate-substrate interactions

The ground-state energy, $e_0(\text{hold})$, of a single helium atom or hydrogen molecule in the holding potential is listed for several adsorbate-substrate combinations in Table II. The energies are derived from resonances observed in selective adsorption scattering experiments. The values for D₂ on graphite and D₂/Ag(111) are based^{2,5} on a combination of data for excited states of those systems and for the H₂ cases, since the ground-state levels of the D₂ systems were not detected in the experiments. The entry for Ne on graphite comes from a calculation¹⁷ for a holding

TABLE II. Adatom-substrate ground-state energy. Energy $e_0(\text{hold})$ in K.

Adsorbate	Substrate		
	Graphite ^a	Ag	Cu
²⁰ Ne	350 ^b		
H ₂	482 ^c	298 ^d	197 ^e
D ₂	516 ^c	316 ^d	
⁴ He	140 ^f	52 ^g	52 ^h
³ He	135 ^f		

^aBasal plane surface of graphite.

^bCalculated, Ref. 17, from a holding potential fitted to gas-surface virial data.

^cReference 2.

^dOn the (111) face of Ag, from Ref. 5.

^eOn the (110) face of Cu, Ref. 4.

^fFrom a review, Ref. 1.

^gOn the (110) face of Ag, Ref. 3.

^hOn Cu(113) and Cu(115), Ref. 4.

potential model fitted to gas-surface virial data.

The ground-state energies⁴ for H₂/Cu(110) and H₂/Cu(115) differ by less than 5%; the ground-state energies⁴ for ⁴He on Cu(113), Cu(115), and Cu(117) differ by about 10%. Thus the experimental value³ for ⁴He/Ag(110) may be close to the value of Ag(111), although registry effects of the adlayer with the substrate depend on which substrate plane is exposed.

The binding energy of a single helium atom on a completed helium monolayer on graphite was derived by Novaco³² from an analysis of adsorption isotherm data: 30.0±0.1 K for ⁴He/⁴He on graphite and 25.4±0.1 K for ³He/³He on graphite. Corresponding information for adsorption of helium on metals, such as the He/Au system,³³ is not yet available.

3. Three-dimensional ground-state properties

The ground-state energy E_{3D} and nearest-neighbor spacing L of the three-dimensional solids of Ne, H₂, and D₂ are listed in Table III. For the helium isotopes, the

TABLE III. Three-dimensional ground state. Cohesive energy in K and nearest-neighbor spacing L in Å.

System	$E(3D)$ (K)	L (Å)	Source
²⁰ Ne	232	3.155	expt. ^a
	-222	3.168	Hartree ^b
	-228	3.159	Jastrow ^c
D ₂	-132.8	3.605	expt. ^d
	-129	3.559	Hartree ^b
	-137	~3.58	Jastrow ^c
H ₂	-89.8	3.789	expt. ^d
	-65.9	3.769	Hartree ^b
	-85.47	3.784	Jastrow ^f
⁴ He	-7.14		liquid, expt. ^g
	-5.95		Jastrow ^h
	0.49	3.67	solid expt. ⁱ
³ He	-2.52		liquid, expt. ^j
	-2.92		Jastrow bosons ^k
	9.70	3.74	solid, expt. ⁱ

^aReference 28.

^bHartree calculation with LJ(12,6) potential of Table I; this work.

^cJastrow variational calculation for LJ(12,6) potential of Table I; Ref. 27.

^dReference 25.

^eAs in c, based on Monte Carlo data of Ref. 26; the separation L for the minimum-energy solid is poorly determined in our calculation and may be accurate to about 1%.

^fAs in c, Ref. 26.

^gFrom Ref. 21, liquid density 0.0218 Å⁻³.

^hFor LJ(12,6) potential of Table I; liquid density 0.0196 Å⁻³, Ref. 41.

ⁱEnthalpy and nearest-neighbor spacing for a solid at the melting curve at zero temperature, Ref. 34.

^jFrom Ref. 21, liquid density 0.0164 Å⁻³.

^kJastrow calculation for LJ(12,6) potential of Table I and bosons of ³He mass, Ref. 41, liquid density 0.0142 Å⁻³.

ground state is a liquid: the entries in Tables III give the number density of the liquid as well as the nearest-neighbor spacing in the solid at the melting curve near 0 K. These data are taken from recent reviews and compilations.^{21,25,28,34}

B. Approximation techniques

The ground-state energy of a near-harmonic solid can be approximated using the zero-point energies of the normal modes determined with harmonic lattice dynamics. The quasiharmonic theory of few-layer systems is the development of this approximation to include two- and three-layer condensation phenomena.³⁵ Results of the quasiharmonic theory for the bilayer condensation of D₂ on graphite are summarized in Appendix B.

When the atomic or molecular motions in the solid are strongly anharmonic and the root-mean-square displacements from lattice sites in the solid are an appreciable fraction of the nearest-neighbor spacing, other approximation methods are necessary to determine the ground-state structure. The Hartree theory^{12-14,36} is based on a self-consistent treatment of noncorrelated displacements from the lattice sites and is a generalization of the Einstein oscillator model of a solid. The quantum-cell theory,¹⁸ based on the Lennard-Jones and Devonshire cell model, is a non-self-consistent version of the Hartree theory. The Jastrow approximation^{10,16,21,29} includes correlation among the motions and is applicable to a quantum liquid as well as to the quantum solid. Both the Hartree and Jastrow theories are variational approximations in quantum mechanics.

In the Hartree and Jastrow theories the basic calculation is to find a variational upper bound on the lowest energy at a prescribed density for the many-body Hamiltonian ($N \rightarrow \infty$):

$$H = -\eta \frac{\epsilon}{2} \sum_{i=1}^N \nabla_i^2 + \frac{1}{2} \sum_{i \neq j} \phi(r_{ij}) . \quad (2.5)$$

For Eq. (2.5) and in the following, lengths are written in units of the LJ(12,6) σ , Eq. (2.1).

1. Hartree theory

The Hartree variational theory requires a functional optimization of the one-body factor ψ in the trial ground-state wave function:

$$\Psi_H = \prod_{i=1}^N \psi(r_i) . \quad (2.6)$$

The nonlinear integral equation for ψ obtained by minimization of the trial energy

$$E_{tH} = \frac{\int d\mathbf{r}_1, \dots, d\mathbf{r}_N \Psi_H^* H \Psi_H}{\int d\mathbf{r}_1, \dots, d\mathbf{r}_N |\Psi_H|^2} \quad (2.7)$$

is

$$-\frac{\eta}{2} \nabla^2 \psi(r_i) + \frac{1}{\epsilon} \sum_{j (\neq i)} \int d\mathbf{r}_j |\psi(r_j)|^2 \phi(r_{ij}) \psi(r_i) = \epsilon_0 \psi(r_i) \quad (2.8)$$

with corresponding energy

$$E_H/(N\epsilon) = \epsilon_0 - \frac{1}{2\epsilon} \frac{\left[\sum_{j \neq 0} \int d\mathbf{r}_j d\mathbf{r}_0 \phi(r_{j0}) |\psi(r_0)|^2 |\psi(r_j)|^2 \right]}{\left[\int d\mathbf{r}_j |\psi(r_j)|^2 \right]^2}. \quad (2.9)$$

We seek solutions $\psi(u)$ which are circularly symmetric (spherically symmetric in three dimensions) in the displacements $\mathbf{u}_j = \mathbf{r}_j - \mathbf{R}_j$ from the lattice sites, in analogy to the Nosanow and Shaw three-dimensional theory.¹² Rosenwald³⁶ included angular dependences reflecting the symmetry of the cell defined by the neighboring sites of the lattice in calculations for the 3D ^3He solid, but the changes in the enthalpy were only 10% relative to the results for the spherically symmetric trial function. With the circularly symmetric ψ and the Lennard-Jones pair potential the angular integrations implicit in the expectation value in Eq. (2.7) can be performed analytically, as in the 3D case.¹²

We also use the Hartree theory for a study of the stability of registry $\sqrt{3}$ lattices of helium and hydrogen on graphite. The Hamiltonian H , Eq. (2.5), then has an additional registry energy term³⁷

$$6V_{g_0} \sum_{j=1}^N J_0(g_0 u_j), \quad (2.10)$$

where g_0 is the shortest nonzero reciprocal-lattice vector, 2.95 \AA^{-1} for graphite, and J_0 is the zeroth-order cylindrical Bessel function.

A further approximation, starting from the Hartree theory, leads to an estimate of an Einstein energy for single-particle excitation. If the relaxation of the neighbors of the excited particle is neglected, the approximate Einstein energy is the difference of the ground-state energy ϵ_0 of Eq. (2.8) and the first excited-state energy ϵ_1 of

the cell potential:

$$-\frac{\eta}{2} \nabla^2 \psi + \frac{1}{\epsilon} \sum_{j (\neq i)} \int d\mathbf{r}_j \phi(r_{ij}) |\psi_0(r_j)|^2 \psi(r_i) = \epsilon_1 \psi. \quad (2.11)$$

In Eq. (2.11), ψ_0 is the ground-state solution of Eq. (2.8); for the $\sqrt{3}$ lattice the registry potential, Eq. (2.10), is added in Eqs. (2.8) and (2.11). In our applications, the first excited state has one unit of angular momentum. The excitation energy $\epsilon(\epsilon_1 - \epsilon_0)$ is related to the mean-square displacement in the ground state, $\langle r^2 \rangle$, by an inequality based on the dipole sum rule in D dimensions:

$$\langle r^2 \rangle \leq D \hbar^2 / [2m\epsilon(\epsilon_1 - \epsilon_0)].$$

The values of $\langle r^2 \rangle$ in the applications of Sec. III are within 3% of this upper bound.

The numerical solution of Eq. (2.8) for two dimensions is with conventional methods. The equation (in the radial variable only) is solved by iteration and Hartree damping, with a solution of the Schrödinger equation within each iteration by the Cooley algorithm.³⁸ Twelve shells of neighbors are included in the potential sums in the self-consistent calculation; the effect of further shells of neighbors is added with a static lattice sum end correction. Grid sizes of fractions 0.01, 0.005, and 0.0025 of the nearest-neighbor spacing are used in the numerical integrations; energies determined with the 0.0025 grid appear to have precision better than 0.01 in E/ϵ and 0.05 in the scaled enthalpies.

Results for the ground state of the two-dimensional

TABLE IV. Monolayer properties. Calculations with Hartree and Jastrow trial functions for the LJ(12,6) models of Table I.

System	Hartree			Jastrow		
	E_0 (K) ^a	L_u (Å) ^a	$L_1(3D)$ (Å) ^b	E_0 (K) ^a	L_u (Å) ^a	$L_1(3D)$ (Å) ^b
Ne on graphite	-78.5	3.282	3.116	-81.0	3.26	e
D ₂ on graphite	-35.3	3.784	3.34	-44.0	3.72	3.33 ^f
D ₂ /Ag(111)	-35.3	3.784	3.46	-44.0	3.72	3.44
H ₂ on graphite	-7.96	4.180	3.45	-22.3	4.07	3.41
H ₂ /Ag(111)	-7.96	4.180	3.58	-22.3	4.07	3.52
⁴ He on graphite	c		3.15	-0.5 ^{c,d}		3.09
⁴ He/Ag(110)	c		3.52	-0.5 ^{c,d}		3.41
³ He on graphite	c		3.27			3.20

^aEnergy (in K) and nearest-neighbor spacing (in Å) of the two-dimensional ground state; no substrate registry effects.

^bMonolayer nearest-neighbor spacing in Å for which the upper bound in Eq. (3.4) is achieved; E_{3D} calculated in the same variational approximation as h_{lat} .

^c2D ground state is a liquid, Refs. 45 and 46.

^dThis work; a more-detailed treatment (Ref. 45) has -0.62 K at 0.037 \AA^{-2} .

^eNo calculation.

^fBy extrapolation (Fig. 1).

(2D) and 3D solids obtained from our solutions for the Lennard-Jones models of Table I are presented in Tables III and IV. In the neon case, which is the only one overlapping with previous workers, our value for the 3D ground-state energy differs from Hansen's value²⁷ by 0.5%; we did not identify the source of this difference.

The quantum-cell-model approximation of recent

$$\frac{-\eta}{2} \nabla^2 \psi(\mathbf{u}) + \left[\frac{1}{2\pi\epsilon} \int_0^{2\pi} d\theta_u \sum_{j \neq 0} [\phi(\mathbf{R}_j + \mathbf{u}) - \phi(R_j)] \right] \psi(\mathbf{u}) = \lambda_0 \psi(\mathbf{u}), \quad (2.12)$$

by

$$E_{QC}/(N\epsilon) = \lambda_0 + \frac{1}{2\epsilon} \sum_{j \neq 0} \phi(R_{j0}). \quad (2.13)$$

An analysis of the relation of this energy to the Hartree energy E_H is given in Appendix A, using a perturbation-variation theory.

2. Jastrow theory

The Jastrow variational theory for a many-boson system has trial functions of the form

$$\Psi_J = \left[\prod_i \psi(u_i) \right] \prod_{i < j} f(r_{ij}). \quad (2.14)$$

We use this trial function in mathematical two dimensions, with the McMillan form²⁹ for the pair factor

$$f(r) = \exp\left[-\frac{1}{2}(b/r)^5\right], \quad (2.15)$$

and two forms for the one-body factor:

$$\psi = 1 \quad (\text{fluid}), \quad (2.16)$$

$$\psi = \exp(-Au^2/2) \quad (\text{solid}).$$

(The wave function for the solid is not fully symmetric.) The formalism is the same as that used by Liu, Kalos, and Chester.¹⁶ The trial energy for the LJ(12,6) potential is

$$E_J/(N\epsilon) = 2 \left[\left\langle \frac{1}{r^{12}} \right\rangle - \left\langle \frac{1}{r^6} \right\rangle \right] + \left[25 \frac{b^5}{8} \eta \right] \left\langle \frac{1}{r^7} \right\rangle + (A\eta/2), \quad (2.17)$$

where the expectation values of the inverse power laws are defined in terms of the pair distribution function by

$$\left\langle \frac{1}{r^j} \right\rangle = \rho^* \int d^2r \frac{1}{r^j} g(r). \quad (2.18)$$

The virial theorem for the spreading pressure p is

$$\frac{p^*}{\rho^*} = \frac{1}{N} \left\langle -\frac{\eta}{2} \sum_{i=1}^N \nabla_i^2 \right\rangle + (-\rho^*/4) \int d^2r g(r) \mathbf{r} \cdot \nabla \phi; \quad (2.19)$$

it remains valid for the pressure derived from variational energies if the length scale in the trial function is optimized.

work^{17,18} for Ne on graphite differs from the theory of Eqs. (2.6)–(2.9) in not having a self-consistent determination of the cell potential and in miscounting part of the interaction energy. The ground-state energy in the quantum-cell (QC) model, for given lattice sites R_j , is obtained from the ground-state solution of the Schrödinger equation,

The expectation values required in Eqs. (2.17) and (2.19) are obtained from primary calculations by McMillan scaling.²⁹ We augmented the tables presented by Liu *et al.*¹⁶ with several more Monte Carlo calculations to extend the variational search to the parameters corresponding to H₂, D₂, and Ne. Most of the new calculations were for Monte Carlo cells of 36 particles and some for 100 particles; the data are presented elsewhere.³⁹ The Monte Carlo expectation values appear to be statistically accurate to 1%; repeating some of the cases treated by Liu *et al.*¹⁶ also gave agreement to 1%. Our Jastrow calculations use a combination of the Liu data and the new data, although there are some irregularities in the combined data set.

The Monte Carlo calculations are based on the correspondence of the expectation values to averages for a classical inverse power-law fluid. It is worth noting that Novaco and Shea⁴⁰ determined the limiting density of the fictitious fluid corresponding to Eq. (2.15) to be

$$\rho^* b^2 \simeq 1.80, \quad (2.20)$$

beyond which the system crystallizes. The largest value of this combination of density and b parameter in our treatment of the fluid phase occurs in the neon case, where the product $\rho^* b^2$ almost reaches 1.5.

The Jastrow ground-state parameters of 3D ²⁰Ne, from Hansen,²⁷ and of H₂, from Bruce,²⁶ are listed in Table III. The Jastrow ground-state energy for 3D D₂ listed there is derived from Bruce's Monte Carlo data.²⁶ The entries for helium are taken from the literature.^{21,34,41}

III. APPLICATIONS

This section is divided into six subsections. The criteria for the limit of monolayer compression are summarized in Sec. III A. The condition for the onset of a quantum liquid as the ground state of a 2D boson system is given in Sec. III B. The results of calculations for neon are given in Sec. III C. Results for the equation of state of the monolayer quantum solid with no substrate registry effects are presented in Sec. III D for hydrogen and in Sec. III E for helium. Calculations on the stability of the $\sqrt{3}R$ 30° lattices of helium and of hydrogen on the basal plane surface of graphite are summarized in Sec. III F.

A. Criteria of the zero-temperature phase equilibria

The conditions of the phase equilibria at zero temperature are stated in terms of the enthalpy h per particle and

the spreading pressure p derived from the internal energy per particle by

$$p = -\partial u / \partial a , \quad (3.1)$$

$$h = u + ap . \quad (3.2)$$

In these equations a is the area per particle and the partial derivative is taken with other structural parameters (e.g., the interlayer spacing) held constant at the values which minimize the energy u for the given a . We use Eq. (3.1) as a check on the internal consistency of calculations with the virial theorem for the pressure, Eq. (2.19). At zero temperature the enthalpy per particle is equal to the chemical potential.

The conditions of mechanical and mass transfer equilibrium between two monolayer phases I and II at zero temperature are

$$p_I = p_{II} , \quad (3.3)$$

$$h_I = h_{II} .$$

Equations (3.3) are equivalent to the Maxwell double tangent construction for first-order phase equilibrium and are used in Sec. III E for the determination of the freezing of two-dimensional (2D) helium.¹⁶

The extent to which the zero-temperature monolayer can be compressed is limited by the formation of three-dimensional (3D) bulk phase with ground-state energy E_{3D} per particle. The ground-state energy in the holding potential $e_0(\text{hold})$, from Table II, and E_{3D} set a bound on the enthalpy arising from adatom-adatom interactions:

$$h_{\text{lat}} \leq E_{3D} - e_0(\text{hold}) . \quad (3.4)$$

A more stringent bound is available when the second-layer condensation energy ϵ_{II} is known:

$$h_{\text{lat}}(\text{bilayer limit}) \leq \epsilon_{II} - e_0(\text{hold}) . \quad (3.5)$$

Equation (3.4) can be applied in the absence of any information on the bilayer structure. As shown in Secs. III C and III E it is informative because the limit on the nearest-neighbor spacing set by Eq. (3.4) does not differ much from that set by Eq. (3.5). For He on graphite, values³² for the binding of a second-layer helium atom to the graphite and first-layer helium are good approximations to ϵ_{II} because the lateral binding-energy terms in the second layer are small.

B. Critical de Boer parameter for onset of a boson liquid ground state

The ground state of a many-body system is a fluid rather than a solid when the confinement kinetic energy is large. The transition occurs when the ground-state energy of the fluid becomes equal to that of the solid, a horizontal tangent in the Maxwell construction. For the 2D many-boson system interacting via LJ(12,6) pair potentials, we find, using the variational trial functions of Eqs. (2.14)–(2.16), that this occurs at

$$\Lambda^* = 2.16 , \quad (3.6)$$

$$\eta = 0.118 .$$

The scaled coexistence densities are $\rho_f^* = 0.375$ and $\rho_s^* = 0.43$, with energy $E^* = -0.222$. The ground state of the 2D solid is so dilated as to become mechanically unstable in the quasiharmonic approximation already⁴² at $\Lambda^* = 0.704$.

For the LJ(12,6) series, with similar trial functions, Nosanow *et al.*¹⁰ found the onset of the boson fluid in three dimensions is at $\Lambda^* = 2.60$, $\eta = 0.171$. Later, Nosanow⁴³ adjusted the calculations so as to reproduce the zero-temperature solidification pressure for helium. The critical de Boer parameter is then displaced to $\Lambda^* = 2.32$, $\eta = 0.136$.

Thus, H₂ physisorbed on a very smooth substrate surface, perhaps Ag(111), is likely to condense at very low temperatures as a solid and not as a quantum liquid, although it would have a low melting temperature.

C. Neon

Monolayer neon was previously treated with quasiharmonic lattice dynamics¹⁷ and with the quantum-cell approximation.^{17,18} We now summarize those results and present the results of the Hartree and Jastrow calculations.

The ground state of the LJ(12,6) Ne in the quasiharmonic approximation has energy -89.4 K and nearest-neighbor spacing $L = 3.288$ Å in two dimensions and energy -237 K and $L = 3.160$ Å in three dimensions. The parameters of the bilayer condensation at zero temperature are (these values are corrections of results reported in Ref. 17) as follows: $L_1 = 3.142$ Å, $L_2 = 3.164$ Å, $z_{12} = 2.55$ Å, $p = 16.3$ K/Å², and chemical potential (enthalpy) $\mu = -295$ K. The ground state of the 2D LJ(12,6) Ne in the quantum-cell approximation has¹⁸ energy -82.7 K at $L = 3.285$ Å.

The ground-state parameters in the Hartree and Jastrow approximations for 2D LJ(12,6) Ne are listed in Table IV. The Hartree energy is -78.5 K at $L = 3.282$ Å, showing that the self-consistency term omitted from the quantum-cell theory is 4 K; this agrees with the perturbation-variation analysis in Appendix A. The minimum Jastrow energy is -81.0 K at $L = 3.26$ Å; that is, the quantum-cell energy contains partially offsetting errors by the omissions of the self-consistency term in the cell potential and of the correlation energy. We believe the size of the difference in the values of L from the Hartree and Jastrow calculations is an artifact of small irregularities in combining our Monte Carlo data with the data of Liu *et al.*¹⁶

The corresponding comparisons for the ground state of 3D LJ(12,6) Ne are energy -222 K at $L = 3.168$ Å in the Hartree calculation and -228 K at $L = 3.159$ Å in Hansen's Jastrow calculation.²⁷

The bound on the monolayer enthalpy set by the 3D cohesive energy, Eq. (3.4), is reached for a monolayer $L = 3.116$ Å, which is 1% smaller than that set by the quasiharmonic theory of bilayer condensation. If the quasiharmonic value for ϵ_{II} is used in Eq. (3.5) as a limit on the lateral enthalpy from the Hartree approximation, the limit on the monolayer lattice constant is 3.158 Å, 1.4% larger than the value from Eq. (3.4) and 0.5% larger than the value from the quasiharmonic theory. The 2D

Hartree theory thus leads to estimates of 5% monolayer compression before bulk formation and 4% compression before bilayer formation. The difference from the use of Eqs. (3.4) and (3.5) is more significant here than in Secs. III D and III E where the net range of compression is larger, but this analysis does specify the lattice constant of the strongly compressed monolayer to 1%. Equation (3.4) sets an informative limit on the monolayer lattice constant because the enthalpy is a rapidly varying function of lattice constant in the strongly compressed monolayer.

D. H₂ and D₂

Results for the LJ(12,6) ground state of D₂ and of H₂ are presented in Table III for the three-dimensional (3D) solid and in Table IV for the two-dimensional (2D) solid. The 3D H₂ Jastrow results were obtained by Bruce,²⁶ while the 3D D₂ Jastrow results are from our calculations with Bruce's Monte Carlo data.²⁶ The large difference between the ground-state parameters of H₂ calculated with the Hartree and the Jastrow approximations in three dimensions also appears in the results for two dimensions. As expected, these differences are smaller for the ground state of D₂.

Monolayers of H₂ and D₂ on the basal plane surface of graphite are observed⁷ to condense as $\sqrt{3}R30^\circ$ lattices and to compress as triangular lattices to limiting values of the nearest-neighbor spacings L of 3.51 Å for H₂ and 3.40 Å for D₂.

The calculations lead to estimates of the energies at the condensation and of the limit set on the monolayer compression by the chemical potential of the ground-state 3D solids, Eq. (3.4). They also show changes in the monolayer limit for adsorption on Ag(111), for which the holding potential is not as deep as on graphite.^{2,5}

The lattice constant of the ground state of 2D LJ(12,6) H₂ is within 5% of the 4.26-Å spacing of the $\sqrt{3}$ lattice on graphite; the difference in the Jastrow energy between the minimum-energy lattice and the $\sqrt{3}$ lattice is only 0.6 K/molecule. Thus, small amplitudes V_g , Eq. (2.10), for periodic components of the molecule-graphite potential may suffice to stabilize the $\sqrt{3}$ lattice; this is discussed further in Sec. III F. The ground state of the unmodulated 2D liquid has energy -16.3 K/molecule and is unstable relative to the solid.

The lattice constant of the ground state of 2D LJ(12,6) D₂ is 12% less than the spacing in the $\sqrt{3}$ lattice. The minimum-energy solid has a Jastrow energy 9 K/molecule lower than that of the liquid. This solid has Jastrow energy 9 K/molecule lower than that of a solid at the $\sqrt{3}$ density, without the registry potential.

We use the Hartree and Jastrow approximations for the enthalpy as a function of lattice constant to estimate limits for the monolayer compression, with Eq. (3.4). The enthalpies are shown in Fig. 1 and the limits on the monolayer lattice constant are listed in Table IV. The Jastrow value is 3% smaller than the experimental value⁷ for H₂ on graphite and 2% smaller than the experimental value for D₂ on graphite; the Jastrow values from Eq. (3.5) would be larger than the values in Table IV. The monolayers condense in $\sqrt{3}$ lattices with $L=4.26$ Å, so that

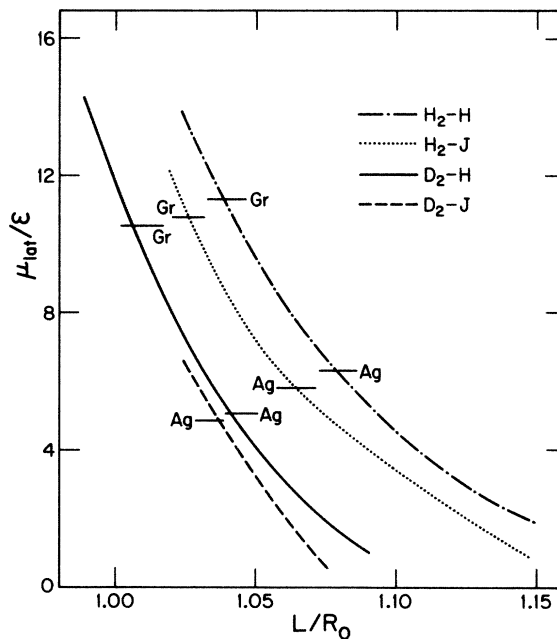


FIG. 1. Reduced lateral enthalpy $\mu_{\text{lat}}/\epsilon$ as a function of the reduced lattice constant L/R_0 of 2D triangular lattices at zero temperature. The curves are the results of Hartree (*H*) and Jastrow (*J*) calculations for LJ(12,6) potentials with the parameters for D₂ and H₂ listed in Table I. The horizontal lines labeled Ag and Gr denote compression limits set by the formation of 3D solid, using data of Table III and of Table II for the holding potentials on Ag(111), Ref. 5, and on basal plane graphite, Ref. 2.

this method of estimating the limit of compression gives the limit on L for the H₂ on graphite to 0.1 Å, with an observed range of 0.75 Å and for D₂ on graphite to 0.05 Å, with an observed range of 0.85 Å. These are quite satisfactory estimates considering the simplicity of the interaction models and the idealization to two dimensions in the calculation.

The entries in Table IV for the adsorption on Ag(111) show changes of 0.1 Å, relative to the values on graphite, in the nearest-neighbor spacings of the limiting monolayers of D₂ and H₂. These changes are a direct consequence of the 200-K difference in the single-molecule ground-state energy on Ag(111) and graphite.

E. ⁴He and boson ³He

Results for the LJ(12,6) model for ⁴He and for bosons of ³He mass are presented in Tables III, IV, and V. The Jastrow-theory values for 3D helium are the results of Schiff and Verlet;⁴¹ further calculations on ⁴He with the LJ(12,6) model²² and with more modern potentials are available.²³ The many-boson theory for ⁴He is easily applied with the ³He mass; it treats fermion exchange effects for ³He incorrectly, but may give a fair account of the enthalpy of compressed monolayer solid ³He.

There were several treatments^{13,14,21,44-46} of monolayer He on graphite prior to the determination¹ of the holding potential by atom-surface scattering experiments. Our results for the compressed monolayer solids show the

changes which follow from the use of the new information and from a somewhat more complete evaluation of the 2D Jastrow theory; there is now a quite close agreement with the low-temperature chemical potential as a function of density derived from thermodynamic data by Goodstein and co-workers.^{47,48} The results in Table V for the freezing transition of the 2D LJ(12,6) boson system extend the work of Liu *et al.*¹⁶

Thermodynamic measurements⁴⁹ gave values for the (low-temperature) high-density limit of monolayer ⁴He on graphite of 0.115 \AA^{-2} ($L=3.17 \text{ \AA}$) and for ³He on graphite of 0.108 \AA^{-2} ($L=3.27 \text{ \AA}$). These values are close to neutron diffraction data: $L=3.21 \text{ \AA}$ for ⁴He at 1.2 K (Ref. 19) and $L=3.275 \text{ \AA}$ for ³He at 1.06 K (Ref. 50).

The difference between the Jastrow and Hartree approximations to the enthalpy, shown in Fig. 2, mostly amounts to an offset of 2% to 3% in the length scale (0.05 to 0.1 \AA in L) in the range of strong compression. Novaco's work¹³ provides a guide to the magnitude of the changes when the motion perpendicular to the graphite is included; there is about a 1% shift in L for enthalpies near the monolayer limit.

The limit on monolayer compression set by the 3D bulk condensation, Eq. (3.4), is listed for ⁴He and boson ³He in Table IV. The information³¹ on ϵ_{II} , summarized in Sec. II A 2 and used with Eq. (3.5), leads to limits set by bilayer condensation of $L=3.17 \text{ \AA}$ for ⁴He on graphite and 3.26 \AA for ³He on graphite. The differences from Novaco's work¹⁴ are primarily consequences of the change¹ in the value for the adatom-substrate binding energy.

Goodstein and co-workers^{47,48} constructed the chemical potential of the compressed He on graphite monolayer from vapor-pressure and specific-heat data. Their low-temperature data and the results of the 2D Hartree and Jastrow calculations are shown in Fig. 3. The results of the Jastrow theory for 2D Lennard-Jones helium, using the one-atom holding energy on graphite taken from scattering data,¹ are in remarkably good agreement with the experimental data for the chemical potential of the compressed monolayers of He on graphite. This supports the neglect of fermion exchange processes in the approximation for the dense 2D ³He solid.

The calculated monolayer limit for ⁴He/Ag(110), assuming an intrinsic 2D triangular lattice, is included in

TABLE V. Freezing parameters at zero temperature of a 2D LJ(12,6) boson fluid. Scaled variables defined in Eqs. (2.2) and (2.4).

Λ^*	2.67	3.08
ϕ^{*a}	0.14	0.31
μ^{*b}	0.39	1.06
ρ_f^{*c}	0.37	0.35
ρ_s^{*d}	0.44	0.43

^aSpreading pressure.

^bChemical potential (enthalpy).

^cDensity of fluid at coexistence.

^dDensity of solid at coexistence.

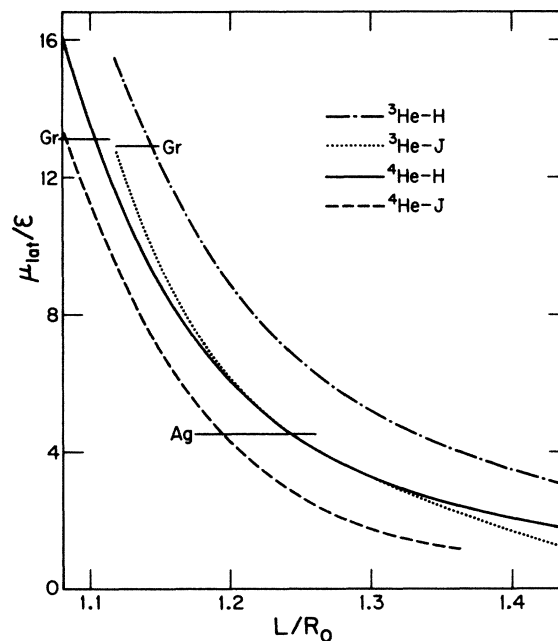


FIG. 2. Reduced lateral enthalpy as a function of the reduced lattice constant, for Lennard-Jones helium. Identifications are as in Fig. 1. Data for the holding potentials are taken from Ref. 1 for graphite and from Ref. 3 for Ag(110). The fermion exchange effects for ³He are omitted and the Jastrow energies, Table III, of the 3D liquid are used for the 3D cohesive energy.

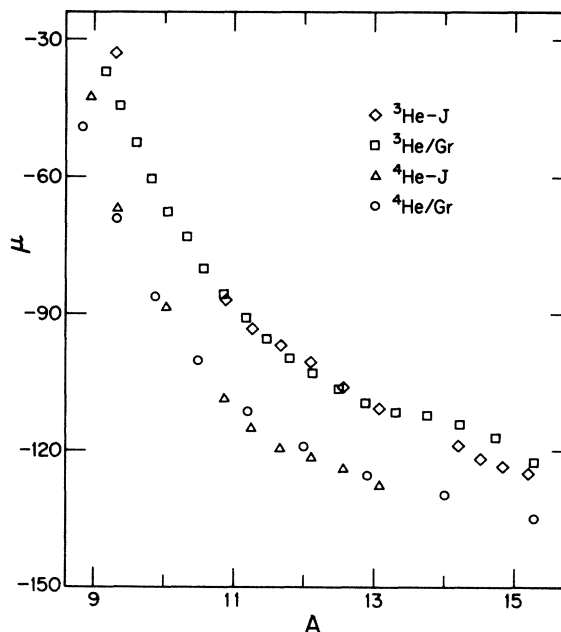


FIG. 3. Chemical potential μ (in K) as a function of area A per particle (in \AA^2) for monolayer ³He on graphite and ⁴He on graphite. The data for ⁴He (\circ) are the values for zero temperature listed by Taborek and Goodstein, Ref. 47; for ³He (\square), they are values for $T < 1 \text{ K}$ from the tabulation of Greif, Ref. 48. The calculated values, denoted (\triangle) for ⁴He and (\diamond) for ³He, are the zero-temperature 2D Jastrow results for triangular lattices, shown in Fig. 2, with the single-adatom ground-state energies, from Ref. 1, added.

Table IV, to show the effect of the weaker adatom/substrate binding relative to graphite. The limit on the nearest-neighbor spacing set by 3D condensation is 10% larger than for graphite, but it is still 7% smaller than that in the 3D solid at the melting curve at zero temperature.³⁴

We also extended calculations¹⁶ of the freezing transition of a 2D boson fluid. The parameters for the freezing transitions of LJ(12,6) ⁴He and boson ³He are listed, in the scaled variables of Eq. (2.4), in Table V. The ⁴He results differ slightly from those of Liu *et al.*;⁶ the changes arise in the Jastrow energy of the solid near the melting density. Note^{10,43} that the corresponding calculation⁵¹ for ⁴He in three dimensions leads to a small melting pressure and to an increase in chemical potential from fluid condensation to freezing of $\Delta\mu^* = 0.3$, which is much smaller than the experimental value³⁴ $\Delta\mu^* = 0.75$.

F. $\sqrt{3}$ -registry lattices on graphite

The low-temperature monolayer condensations of D₂, H₂, ⁴He, and ³He on the basal plane surface of graphite are all^{7,49} into $\sqrt{3}R30^\circ$ lattices stabilized by laterally periodic components³⁷ of the adatom-substrate interaction. The theory of the stability of these registry lattices relative to intrinsic incommensurate lattices is complicated by the limited knowledge of the amplitudes V_g of the periodic components of the holding potential and by the large zero-point motions of the atoms and molecules in quantum monolayer solids.

Here we summarize calculations performed with values for the leading Fourier amplitude V_{g_0} on graphite ($g_0 = 2.95 \text{ \AA}^{-1}$) of -6.4 K for ⁵² H₂ and D₂ and -3.3 K for ¹ ³He and ⁴He. The registry energy, Eq. (2.10), is included in the Hartree calculations with Eqs. (2.8) and (2.11). In the Jastrow calculations, we evaluate the expectation value of the registry energy in the trial function with parameters optimized first at the $\sqrt{3}$ density with no registry potential; this amounts to using first-order perturbation theory for the contribution of the registry potential. As noted in the discussion later in this section, the perturbation calculation of the registry potential with this Jastrow trial function leads to a small net expectation value, because of the large zero-point motions. We believe that the expectation value would be larger for a calculation in which the registry energy is included in the optimization of the Jastrow parameters. However, except for some exploratory calculations for H₂ on graphite, to test this idea, we do not perform this reoptimization. When the registry potential is included in the Jastrow variational calculation the advantages of the McMillan scaling procedure are mostly lost, and the calculations should then be performed with more realistic pair-potential models.

The root-mean-square displacements and the expectation values of the registry potential for the $\sqrt{3}$ lattices, calculated with the Hartree and Jastrow perturbation approximations, are listed in Table VI. In all the cases the root-mean-square displacements are larger in the Jastrow approximation than in the Hartree approximation. For Lennard-Jones ⁴He in three dimensions, the nominally exact root-mean-square displacements calculated by

Whitlock *et al.*²² are up to 10% larger than those calculated with the Jastrow approximation by Hansen and Levesque⁵¹ (after correction²²).

For H₂ on graphite, the difference in 2D energy between the unmodulated minimum energy lattice and the $\sqrt{3}$ lattice density is only 0.6 K/molecule, as noted in Sec. III D. The energy lowering by the periodic potential term, Table VI, greatly exceeds this and should suffice to stabilize the $\sqrt{3}$ lattice. There are also calculations by Wang *et al.*⁵³ for H₂ on graphite at the $\sqrt{3}$ -lattice density. Their models differ from ours, so that detailed comparisons are not possible, but they seem to obtain about 6 K more cohesive energy for the liquid and solid phases than we do (allowing for the difference in values of V_{g_0} and using the Hartree expectation value of the registry energy).

For D₂ on graphite, the 2D Jastrow energy of the minimum-energy solid, Table IV, is 9 K/molecule lower than at the $\sqrt{3}$ density. The additional registry energy in the Hartree approximation, for $V_{g_0} = -6.4 \text{ K}$, is -20 K/molecule and outweighs this difference; however, the corresponding energy from the Jastrow perturbation calculation is -8.8 K . It is likely that the results of a reoptimized Jastrow calculation would be that the $\sqrt{3}$ lattice is also the ground state for the LJ(12,6) model of D₂ on graphite.

We estimate the Einstein excitation energy^{7,15} of the $\sqrt{3}$ lattices of D₂ on graphite and H₂ on graphite with the approximation of Eq. (2.11). The neglect of relaxation and of correlated displacements are likely to be better approximations for D₂ than for H₂. The effect of the periodic potential in the calculation is small: The excitation energy for D₂ on graphite is 46 K for $V_{g_0} = -6.4 \text{ K}$ and 39 K for $V_{g_0} = 0$; for H₂ on graphite the values are 77 K for $V_{g_0} = -6.4 \text{ K}$ and 70 K for $V_{g_0} = 0$. The D₂ on graphite estimate is in good agreement with a value 47 K from neutron scattering experiments,⁷ while the H₂ on graphite estimate is substantially larger than the value 57 K from neutron scattering⁷ and values near 55 K from specific-heat measurements.¹⁵ The excitation energy to the first excited state of single-molecule motion perpen-

TABLE VI. Properties of $\sqrt{3}$ adlayer lattice on graphite. Calculations for LJ(12,6) models of Table I. The root-mean-square displacement is given in units of the nearest-neighbor distance ($L = 4.26 \text{ \AA}$) and the expectation value (in K) of the registry potential uses $V_{g_0} = -6.4 \text{ K}$ for H₂ and D₂, Ref. 52, and $V_{g_0} = -3.3 \text{ K}$ for He, Ref. 1.

	$\langle r^2 \rangle^{1/2}/L$		$\langle V_g(r) \rangle$ (K)	
	H ^a	J ^b	H ^a	J ^b
D ₂	0.12	0.19	-20.2	-8.8
H ₂	0.13	0.20	-18.4	-7.5
⁴ He	0.15	0.26	-6.7	-1.3
³ He	0.16	0.27	-6.4	-1.2

^aHartree (boson) wave function, including the registry potential in the determination of the one-body wave function.

^bJastrow trial function with parameters to minimize the energy of $\sqrt{3}$ lattice without registry potential.

dicular to the substrate is 175 K for H₂ on graphite and 105 K for H₂/Ag(111).⁵ A gap remains between such states and 2D excited states of the monolayer.

For He on graphite the amplitude $V_{g_0} = -3.3$ K derived from atom-surface scattering experiments¹ is twice the value used in early calculations^{44,46} on the stability of the $\sqrt{3}R30^\circ$ lattice. The Hartree-values in Table VI for the lowering of the 2D energy per atom of the $\sqrt{3}$ lattice with amplitude $V_{g_0} = -3.3$ K are about $\frac{1}{3}$ of the classical value of -19.8 K. The net Hartree energies are still positive, but if the Hartree expectation values are combined with the 2D Jastrow solid energies at the $\sqrt{3}$ density, 0.65 K/atom for ⁴He and 3.3 K/atom for ³He, the $\sqrt{3}$ lattices have lower energies than the unmodulated fluid phases. This would not be the case for ³He with the value $V_{g_0} = -1.56$ K used in earlier work.^{44,46} However, the Jastrow perturbation calculation of the expectation value gives much smaller values, Table VI, then the Hartree calculation so that the stability of the $\sqrt{3}$ lattices of He on graphite has not been established. The root-mean-square vibrations of helium atoms in the $\sqrt{3}$ lattice, Table VI, are large: If the atoms were uniformly distributed over a disk of radius $L/2$, the root-mean-square displacement would be $0.354L$.

Einstein excitation energies for the 2D model of the $\sqrt{3}$ lattice, calculated with $V_{g_0} = -3.3$ K and Eq. (2.11), are 28 K for ⁴He on graphite and 35 K for ³He on graphite (24 and 31 K with $V_{g_0} = 0$). As for H₂ on graphite, the neglect of relaxation and correlation may cause these values to be significantly larger than those which would result from a more complete theory. Even so, they are much less than the excitation energy of motion perpendicular to the substrate,¹ 66 K for ⁴He on graphite and 72 K for ³He on graphite, and a sizable gap remains between the energy of 2D motion and of perpendicular motion. The gap would be smaller for ⁴He/Ag(110) and ⁴He/Cu where the excitation energy for perpendicular motion is^{3,4} about 25 K. Decoupling perpendicular and parallel motions would be a particularly severe approximation for adsorption on hydrogen films where the ground-state energy in the holding potential is calculated⁹ to be smaller than 20 K.

IV. CONCLUDING REMARKS

Although there were several previous treatments of the quantum mechanics of monolayer helium, our work still has the character of exploratory calculations. The simplified interaction models and idealized (2D) geometry lead, nevertheless, to nearly quantitative accounts of the limiting compressed monolayer states of helium and of hydrogen, before further condensations. The advances in knowledge of atom-surface and molecular-surface interactions provide a much improved basis for understanding the structures at monolayer condensation and at monolayer completion for light adsorbates with large quantum effects. The quantum monolayers arise in the study of spin-polarized 3D ³He as well as directly in the extension of physisorption studies; they have a role in the theory of layer-growth phenomena. Their structures may be acces-

sible with extensions of methods used to probe more classical monolayers.

ACKNOWLEDGMENTS

This work was supported in part by the National Science Foundation through Grant No. DMR-8214518. We are grateful to Professor J. M. Phillips for supplying us with a Monte Carlo program which was central to our Jastrow variational calculations. This work is based on a Ph.D thesis submitted by X.-Z. Ni in partial fulfillment of the requirements for the Doctor of Philosophy degree, University of Wisconsin-Madison, 1985.

APPENDIX A: PERTURBATION-VARIATION APPROXIMATION TO THE HARTREE AND QUANTUM-CELL THEORIES

We outline a near-harmonic approximation to the ground state of the Hamiltonian of Eq. (2.5) which has good accuracy, compared to the detailed solution of the Hartree theory, for Ne and for compressed lattices of D₂.

For this purpose, rewrite the potential-energy term of Eq. (2.5) using the displacements \mathbf{u}_i from lattice sites \mathbf{R}_i ($\mathbf{R}_{ij} = \mathbf{R}_i - \mathbf{R}_j$):

$$\Phi = \sum_{i < j} \phi(|\mathbf{R}_{ij} + \mathbf{u}_i - \mathbf{u}_j|). \quad (\text{A1})$$

Then expand in powers of the displacements, retaining terms up to the sixth order in products of \mathbf{u}_i and \mathbf{u}_j . The expansion greatly simplifies when circular (spherical for three dimensions) averages over orientations of the displacement vectors are performed; this corresponds to using the symmetry assumed for the Hartree trial function and to the averaging performed on the cell potential of the quantum-cell model, e.g., Eq. (2.12).

The Hartree energy E_H and the quantum-cell energy E_{QC} are then give in terms of expansion coefficients:

$$\begin{aligned} \Phi_0 &= \frac{1}{2} \sum_j \phi(R_j), \\ A &= \frac{1}{2} \sum_j \nabla^2 \phi(R_j), \\ B &= \frac{1}{24} \sum_j \nabla^2 \nabla^2 \phi(R_j), \\ C &= \frac{1}{720} \sum_j \nabla^2 \nabla^2 \nabla^2 \phi(R_j), \end{aligned} \quad (\text{A2})$$

and averages of the displacements \mathbf{u} with normalized single-particle wave functions $\psi(\mathbf{u})$,

$$\langle u^n \rangle = \int d\mathbf{u} |\mathbf{u}|^n |\psi(\mathbf{u})|^2 \quad (\text{A3})$$

by

$$\tilde{E}_H/N = \tilde{E}_{QC}/N + e_{sc} \quad (\text{A4})$$

with

$$\begin{aligned} \tilde{E}_{QC}/N &= \Phi_0 + \frac{\hbar^2}{2m} \int d\mathbf{u} |\nabla \psi|^2 \\ &+ [(A/D)\langle u^2 \rangle + Bf\langle u^4 \rangle + Cg\langle u^6 \rangle] \end{aligned} \quad (\text{A5})$$

and

$$e_{sc} = (3B/D^2)\langle u^2 \rangle^2 + (15Cf/D)\langle u^2 \rangle \langle u^4 \rangle. \quad (\text{A6})$$

The numerical factors f and g in D dimensions are $f = \frac{3}{8}$ and $g = \frac{5}{16}$ for $D=2$ and $f = \frac{1}{5}$ and $g = \frac{1}{7}$ for $D=3$. This completes the statement of the perturbation portion of the perturbation-variation theory.

For the variation portion use a trial function of the form

$$\psi_t = N_t \exp(-\alpha u^2/2)[1 + a(\alpha u^2) + b(\alpha u^2)^2], \quad (\text{A7})$$

with

$$\alpha = m\omega_E/\hbar, \quad (\text{A8})$$

$$\omega_E^2 = 2A/(mD), \quad (\text{A9})$$

where a and b are variational coefficients, N_t is a normal-

ization factor, and ω_E is the Einstein oscillator frequency for uncorrelated small-amplitude vibrations in the lattice. The trial function incorporates the ground-state wave function of the Einstein oscillator and terms reflecting the first and second excited states of the Einstein oscillator. With the trial function, Eq. (A7), the expectation values in Eqs. (A5) and (A6) reduce to Gaussian integrals and the energies \bar{E}_H and \bar{E}_{QC} are ratios of polynomials in the coefficients a and b . To find the minimum of the variation-perturbation energies $E_H(pv)$ and $E_{QC}(pv)$ is a rapid computation.

When the expansion of the potential energy is truncated at quadratic terms the result is equivalent to the harmonic Einstein oscillator approximation to the ground-state energy, as noted by Nosanow and Shaw.¹² A direct perturbation treatment equivalent to the expansions used in arriving at Eq. (A5) leads⁵⁴ to a ground-state energy $E_{QC}(\text{pert})$ in the quantum-cell approximation,

$$E_{QC}(\text{pert})/N = \begin{cases} \Phi_0 + \hbar\omega_E + [2(Bf/\alpha^2) + 6(Cg/\alpha^3)] - 9[(Bf/\alpha^2)^2/\hbar\omega_E], & D=2 \\ \Phi_0 + \frac{3}{2}\hbar\omega_E + [\frac{15}{4}(Bf/\alpha^2) + \frac{105}{8}(Cg/\alpha^3)] - \frac{165}{8}[(Bf/\alpha^2)^2/\hbar\omega_E], & D=3 \end{cases} \quad (\text{A10})$$

with α and ω_E given by Eqs. (A8) and (A9).

For the Ne LJ(12,6) model, Table I, the values of $E_H(pv)$ are very close to E_H , the numerical solution of the Hartree equation, Sec. III. The ground-state parameters differ by only 0.008 in E/ϵ and 0.002 in L/R_0 for both $D=2$ and $D=3$. The scaled enthalpy obtained from $E_H(pv)$ differs from that for the detailed numerical solution by about 0.01 at lattice constants L/R_0 in the range of monolayer completion; this has negligible effect in estimating the limiting value of the monolayer lattice constant L . The difference $E_{QC}(pv) - E_H(pv)$, for lattice constants near the ground state, is about 0.11ϵ (4 K) for $D=2$ and about 0.15ϵ (5.5 K) for $D=3$.

For the D_2 LJ(12,6) model, Table I, the $D=3$ $E_H(pv)/\epsilon$ value differs from E_H/ϵ by 0.05 for $L/R_0=1.075$, near the calculated minimum-energy Hartree state; the accuracy is better for more compressed lattices. For the $D=2$ cases, the difference $[E_H(pv) - E_H]/\epsilon$ is 1.2 at $L/R_0=1.10$ and is smaller than 0.1 at $L/R_0=1.06$; again the accuracy is better for the compressed lattice. The perturbation theory value, Eq. (A10), is very different from E_H in magnitude and in variation with lattice constant for values of L/R_0 where $E_H(pv)$ is close to E_H .

The trial function Eq. (A7) can be generalized to include the scale α of the Gaussian as a variational parameter, rather than specifying it by Eqs. (A8) and (A9). However, when the generalized $E_H(pv)$ is compared to E_H , there are only small changes for Ne (less than 0.001ϵ). For D_2 , there are sizable changes, but no definite improvement in the approximation for the enthalpy of the dilated lattice.

APPENDIX B: QUASIHARMONIC THEORY OF THE BILAYER CONDENSATION OF D_2 ON GRAPHITE

In this appendix we summarize an application of the quasiharmonic theory of multilayer condensation³⁵ to the bilayer condensation of D_2 on graphite. The quasiharmonic approximation has instabilities at high levels of thermal excitation and when the interplanar spacings of bilayers and trilayers become large. This has prevented application to the H_2 on graphite bilayer condensation and to the question of a trilayer condensation for D_2 on graphite. For a D_2 on graphite bilayer composed of triangular lattice layers, we are able to find local free-energy minima as a function of the interlayer spacing.

We use the LJ(12,6) potential of Table I, supplemented by the following parameters for the D_2 on graphite interaction: The reference plane for the polarization potential is chosen so that the minimum of the one-molecule holding potential is at a distance 1.45 Å from the "surface;" the polarization potential coefficient has a value of $C_3=0.121$ a.u.; the holding potential minimum has a depth of 51.54 meV and curvature of $216 \text{ meV}/\text{Å}^2$.

The calculated zero-temperature coexistence of the triangular monolayer and bilayer is at chemical potential -237 K and spreading pressure $32.6 \text{ K}/\text{Å}^2$ with lateral nearest-neighbor spacing 3.359 Å in the monolayer and 3.440 Å in the bilayer. The bilayer has interplanar spacing 2.839 Å and first overlayer distance 1.428 Å. The reduced lateral energy contribution to the enthalpy, Eq. (3.5), is $h_{\text{lat}}/\epsilon=3.07$, while the bound from Eq. (3.4) us-

ing the experimental data of Tables II and III is $h_{\text{lat}}/\epsilon < 5.91$.

We also considered a possible coexistence of triangular monolayer and oblique lattice bilayer, because of proposals that a reorganization of the close-packed bilayer into a looser oblique structure might occur for light adsor-

bates.¹⁹ However, the search for local free-energy minima in the quasiharmonic approximation led to lattices with unstable harmonic phonons.⁴² The possibility that zero-point energy and anisotropic components²⁵ of the intermolecular forces may stabilize an oblique bilayer lattice of D_2 remains an open question.

- ¹M. W. Cole, D. R. Frankl, and D. L. Goodstein, *Rev. Mod. Phys.* **53**, 199 (1981).
- ²L. Mattera, F. Rosatelli, C. Salvo, F. Tommasini, U. Valbusa, and G. Vidali, *Surf. Sci.* **93**, 515 (1980).
- ³A. Luntz, L. Mattera, M. Rocca, F. Tommasini, and U. Valbusa, *Surf. Sci.* **120**, L447 (1982).
- ⁴J. Perreau and J. Lapujoulade, *Surf. Sci.* **122**, 341 (1982).
- ⁵C.-F. Yu, K. B. Whalley, C. S. Hogg, and S. J. Sibener, *J. Chem. Phys.* **83**, 4217 (1985).
- ⁶J. G. Dash, *Films on Solid Surfaces* (Academic, New York, 1975).
- ⁷M. Nielsen, J. P. McTague, and W. Ellenson, *J. Phys. (Paris) Colloq.* **38**, C4-10 (1977).
- ⁸R. Pandit, M. Schick, and M. Wortis, *Phys. Rev. B* **26**, 5112 (1982); R. J. Muirhead, J. G. Dash, and J. Krim, *ibid.* **29**, 5074 (1984); J. A. Venables, G. D. T. Spiller, and M. Hanbücken, *Rep. Prog. Phys.* **47**, 399 (1984); F. T. Gittes and M. Schick, *Phys. Rev. B* **30**, 209 (1984).
- ⁹L. Pierre, H. Guignes, and C. Lhuillier, *J. Chem. Phys.* **82**, 496 (1985); V. Lefèvre-Seguin, P. J. Nacher, J. Brossel, W. N. Hardy, and F. Laloë, *J. Phys. (Paris)* **46**, 1145 (1985).
- ¹⁰L. H. Nosanow, L. J. Parish, and F. Pinski, *Phys. Rev. B* **11**, 191 (1975); M. D. Miller, L. H. Nosanow, and L. J. Parish, *ibid.* **15**, (1977).
- ¹¹M. D. Miller and L. H. Nosanow, *J. Low. Temp. Phys.* **32**, 145 (1978).
- ¹²L. H. Nosanow and G. L. Shaw, *Phys. Rev.* **128**, 546 (1962).
- ¹³A. D. Novaco, *Phys. Rev. A* **8**, 3065 (1973).
- ¹⁴A. D. Novaco, *Phys. Rev. A* **7**, 678 (1973).
- ¹⁵F. Motteler and J. G. Dash, *Phys. Rev. B* **31**, 346 (1985); F. A. B. Chaves, M. E. B. P. Cortez, R. E. Rapp, and E. Lerner, *Surf. Sci.* **150**, 80 (1985).
- ¹⁶K. S. Liu, M. H. Kalos, and G. V. Chester, *Phys. Rev. B* **13**, 1971 (1976); **17**, 4479(E) (1978).
- ¹⁷L. W. Bruch, J. M. Phillips, and X.-Z. Ni, *Surf. Sci.* **136**, 361 (1984).
- ¹⁸J. M. Phillips and L. W. Bruch, *J. Chem. Phys.* **79**, 6282 (1983).
- ¹⁹K. Carneiro, L. Passell, W. Thomlinson, and H. Taub, *Phys. Rev. B* **24**, 1170 (1981); H. Taub (private communication).
- ²⁰J. de Boer and A. Michels, *Physica* **5**, 945 (1939).
- ²¹C.-W. Woo, in *The Physics of Liquid and Solid Helium*, edited by K. H. Bennemann and J. B. Ketterson (Wiley, New York, 1976), Vol. 1.
- ²²P. A. Whitlock, D. M. Ceperley, G. V. Chester, and M. H. Kalos, *Phys. Rev. B* **19**, 5598 (1979).
- ²³M. H. Kalos, M. A. Lee, P. A. Whitlock, and G. V. Chester, *Phys. Rev. B* **24**, 115 (1981).
- ²⁴L. A. Michels, W. de Graaff, and C. A. ten Seldam, *Physica* **26**, 393 (1960).
- ²⁵I. F. Silvera, *Rev. Mod. Phys.* **52**, 393 (1980).
- ²⁶T. A. Bruce, *Phys. Rev. B* **5**, 4170 (1972); we note that in using Bruce's Monte Carlo data we arrive at a slightly different ground-state energy, -84.5 K for the parameters of Table I, than he obtained for solid H_2 .
- ²⁷J.-P. Hansen, *Phys. Rev.* **172**, 919 (1968).
- ²⁸G. T. McConville, *J. Chem. Phys.* **60**, 4093 (1974).
- ²⁹W. L. McMillan, *Phys. Rev.* **138**, A442 (1965).
- ³⁰L. W. Bruch, *Surf. Sci.* **125**, 194 (1983), and references contained therein.
- ³¹P. R. Kubik, W. N. Hardy, and H. Glattli, *Can. J. Phys.* **63**, 605 (1985).
- ³²A. D. Novaco, *J. Low Temp. Phys.* **21**, 359 (1975), and references contained therein.
- ³³A. D. Migone, J. Krim, J. G. Dash, and J. Suzanne, *Phys. Rev. B* **31**, 7643 (1985).
- ³⁴R. K. Crawford, in *Rare Gas Solids*, edited by M. L. Klein and J. A. Venables (Academic, New York, 1977), Vol. 2.
- ³⁵L. W. Bruch and X.-Z. Ni, *Faraday Discuss. Chem. Soc.* (to be published), and references contained therein.
- ³⁶D. Rosenwald, *Phys. Rev.* **154**, 160 (1967).
- ³⁷The amplitudes are those defined by W. A. Steele, *Surf. Sci.* **36**, 317 (1973).
- ³⁸J. W. Cooley, *Math. Comp.* **15**, 363 (1961).
- ³⁹X.-Z. Ni, Ph.D. thesis, University of Wisconsin-Madison, 1985 (unpublished).
- ⁴⁰A. D. Novaco and P. A. Shea, *Phys. Rev. B* **26**, 284 (1982).
- ⁴¹D. Schiff and L. Verlet, *Phys. Rev.* **160**, 208 (1967).
- ⁴²M. S. Wei and L. W. Bruch, *J. Chem. Phys.* **75**, 4130 (1981).
- ⁴³L. H. Nosanow, *J. Low Temp. Phys.* **26**, 613 (1977).
- ⁴⁴A. D. Novaco and C. E. Campbell, *Phys. Rev. B* **11**, 2525 (1975).
- ⁴⁵M. D. Miller, C.-W. Woo, and C. E. Campbell, *Phys. Rev. A* **6**, 1942 (1972).
- ⁴⁶A. D. Novaco, *Phys. Rev. A* **7**, 1653 (1973).
- ⁴⁷R. L. Elgin and D. L. Goodstein, *Phys. Rev. A* **9**, 2657 (1974); P. Taborek and D. Goodstein, *Rev. Sci. Instrum.* **50**, 227 (1979).
- ⁴⁸J. M. Greif, Ph.D. thesis, California Institute of Technology, 1982 (unpublished); R. L. Elgin, J. M. Grief, and D. L. Goodstein, *Phys. Rev. Lett.* **41**, 1723 (1978).
- ⁴⁹M. Bretz, J. G. Dash, D. C. Hickernell, E. O. McLean, and O. E. Vilches, *Phys. Rev. A* **8**, 1589 (1973).
- ⁵⁰R. Feile, H. Wiechert, and H.-J. Lauter, *Phys. Rev. B* **25**, 3410 (1982).
- ⁵¹J.-P. Hansen and D. Levesque, *Phys. Rev.* **165**, 293 (1968).
- ⁵²Z.-C. Guo and L. W. Bruch, *J. Chem. Phys.* **77**, 1417 (1982).
- ⁵³S. C. Wang, L. Senbetu, and C.-W. Woo, *J. Low Temp. Phys.* **41**, 611 (1980).
- ⁵⁴L. W. Bruch and J. M. Phillips, *J. Phys. Chem.* **86**, 1146 (1982).